# EFFICIENT ONE-POT MICROWAVE-ASSISTED SYNTHESIS, CRYSTALLOGRAPHIC, AND SPECTROSCOPIC CHARACTERIZATION OF NOVEL ANTITUMOR AND ANTIMICROBIAL (3E)-5-HYDROXY-1-ISOPROPYL-3-[(5-METHYL-2-THIENYL)METHYLENE]-5-PHENYLPYRROLIDIN-2-ONE**

**E. M. Azmy [1], B. M. Awad [1], H. A. Hefni [1], H. A. Saad [1], A. M. Eltoukhya [1], A. F. Mabied [2,3], Mamoun S. M. Abd El-Kareem [4*], N. Demitri [5]**

*[1] Department of Chemistry at Ain Shams University, Heliopolis, Cairo, Egypt*
*[2] X-Ray Crystallography Lab., Solid State Physics Department, National Research Center, Dokki, Giza, Egypt*
*[3] Department of Basic Sciences, October High Institute of Engineering & Technology-OHI, Giza, Egypt*
*[4] Molecular and Atomic Physics unit., Experimental Nuclear Physics Department, Nuclear Research Center, Egyptian Atomic Energy Authority, Inshas, Cairo, Egypt; e-mail: mamoun_sarhan@yahoo.com*
*[5] Elettra Sincrotrone Trieste, 34149 Basovizza–Trieste, Italy*

*A microwave-assisted, chemoselective synthesis of novel antitumor and antimicrobial (3E)-5-hydroxy-1-isopropyl-3-[(5-methyl-2-thienyl)methylene]-5-phenylpyrrolidin-2-one has been achieved via the solvent-free one-pot reaction of (3E)-3-[(5-methyl-2-thienyl)methylene]-5-phenylfuran-2(3H)-one with isopropylamine. The product is obtained in significant purity and yield under ecofriendly reaction conditions. The microwave technique surpasses conventional thermal heating approaches by accelerating the reaction in a clean, ecofriendly manner that avoids the use of organic or toxic solvents. The structural formula of the product is confirmed by crystallographic and spectroscopic characterization. X-ray single crystal diffraction reveals that the compound crystallizes in an orthorhombic centrosymmetric crystal form, with unambiguous assignment of the E-configuration for the $C_3$–$C_{thienyl}$ bond. The synthesized molecules have two centers of chirality in the hydroxypyrrolidin-2-one ring: 1) the carbon atom attached to nitrogen, the hydroxyl group, and the phenyl ring; 2) the nitrogen atom attached to the carbonyl carbon R3 group, the chiral carbon in the ring, and the covalent bond bearing the lone pair of electrons. The molecular geometry is also optimized using density functional theory calculations, and the results obtained are in good agreement with the experimental data. Evaluation of the biological and medicinal activity of the compound affords similar results to the reference data in antitumor treatment of human colon and breast cells, which can be attributed to the presence of the hydroxyl group, the heterocyclic motifs, and sulfur. Calculation of the molecular electrostatic potential locates the most electrophilic site near the hydroxyl group attached to the heterocyclic ring, which is consistent with the bioactivity results. The frontier molecular orbitals are also determined, finding that the energy difference between highest occupied molecular orbital and lowest unoccupied molecular orbital is −0.15228 eV. A mechanism is proposed in which an intramolecular nucleophilic attack occurs on the carbonyl carbon by the lone pair of electrons on the nitrogen atom, leading to ring closure with proton transfer to oxygen and final formation of the hydroxyl group.*

***Keywords:*** *microwave, chemoselective, hydroxypyrrolidin-2-one, catalyst- and solvent-free, ecofriendly, crystallographic characterization.*

** Full text is published in JAS V. 88, No. 2 (http://springer.com/journal/10812) and in electronic version of ZhPS V. 88, No. 2 (http://www.elibrary.ru/title_about.asp?id=7318; sales@elibrary.ru).

# КРИСТАЛЛОГРАФИЧЕСКАЯ И СПЕКТРОСКОПИЧЕСКАЯ ХАРАКТЕРИЗАЦИЯ ПРОТИВООПУХОЛЕВОГО И АНТИМИКРОБНОГО СОЕДИНЕНИЯ (3E)-5-ГИДРОКСИ-1-ИЗОПРОПИЛ-3-[(5-МЕТИЛ-2-ТИЕНИЛ)МЕТИЛЕН]-5-ФЕНИЛПИРРОЛИДИН-2-ОНА

**E. M. Azmy [1], B. M. Awad [1], H. A. Hefni [1], H. A. Saad [1], A. M. Eltoukhya [1], A. F. Mabied [2,3], Mamoun S. M. Abd El-Kareem [4*], N. Demitri [5]**

*УДК 543.42;548.0*

*[1] Университет Айн-Шамс, Гелиополис, Каир, Египет*
*[2] Национальный исследовательский центр, Докки, Гиза, Египет*
*[3] Октябрьский высший институт инженерии и технологий-ОНІ, Гиза, Египет*
*[4] Центр ядерных исследований, Управление по атомной энергии Египта, Иншас, Каир, Египет; e-mail: mamoun_sarhan@yahoo.com*
*[5] Elettra Sincrotrone Trieste, 34149 Басовица-Триест, Италия*

*(Поступила 16 ноября 2019)*

*Синтезировано противоопухолевое и антимикробное соединение (3E)-5-гидрокси-1-изопропил-3-[(5-метил-2-тиенил)метилен]-5-фенилпирролидин-2-он с помощью реакции в одной емкости без растворителя (3E)-3-[(5-метил-2-тиенил)метилен]-5-фенилфуран-2(3H)-она с изопропиламином. Получен продукт с достаточной чистотой и выходом в экологически чистых условиях реакции. Техника микроволн превосходит традиционные подходы к термическому нагреву, ускоряет реакцию чистым и экологичным способом без использования органических или токсичных растворителей. Структурная формула продукта подтверждена кристаллографическими и спектроскопическими исследованиями. Рентгеновская дифракция монокристалла показывает, что соединение кристаллизуется в орторомбической центрально-симметричной кристаллической форме с однозначным назначением E-конфигурации для связи $C_3$–$C_{thienyl}$. Синтезированные молекулы имеют два центра хиральности в кольце гидроксипирролидин-2-она: 1) атом углерода, присоединенный к азоту, гидроксильная группа и фенильное кольцо; 2) атом азота, присоединенный к карбонильному углероду группы R3, хиральный углерод в кольце и ковалентная связь, несущая неподеленную пару электронов. Методом теории функционала плотности рассчитана оптимизированная геометрия молекулы, полученные результаты хорошо согласуются с экспериментальными данными. Оценка биологической и лечебной активности соединения дает результаты, аналогичные исходным данным по противоопухолевому лечению толстой кишки и груди, что может быть связано с присутствием гидроксильной группы, гетероциклов и серы. Расчет электростатического потенциала молекулы определяет местонахождение наиболее электрофильного участка рядом с гидроксильной группой, присоединенной к гетероциклическому кольцу, что согласуется с показателями биоактивности. Определены граничные молекулярные орбитали и обнаружено, что разность энергий между высшей занятой и низшей вакантной молекулярными орбиталями составляет –0.15228 эВ. Предложен механизм, в котором происходит внутримолекулярная нуклеофильная атака на карбонильный углерод неподеленной парой электронов на атоме азота, приводящий к замыканию цикла с переносом протона на кислород и окончательным образованием гидроксильной группы.*

***Ключевые слова:*** *микроволна, гидроксипирролидин-2-он, реакция без катализатора и растворителя, экологичный способ, кристаллографическая характеристика.*

**Introduction.** The heterocyclic motif is an important scaffold with industrial and medicinal applications. Among the diverse heterocyclic compounds, pyrrolidinones possess significant biological and pharmacological activities including anticonvulsant and respiratory stimulation activities. In particular, the 2-pyrrolidinone moiety is very important in medicinal chemistry because many derivatives have shown significant pharmacological and biological activities as anticancer [1, 2] and antitumor agents [3], HIV-1 integrase inhibitors [4, 5], and antimicrobial [6], antibacterial [7], and antiinflammatory drugs [8]. In view of the importance of substituted pyrrolidinones, various synthetic methods have been reported [9–17]. Among those,



ıve-assisted techniques stand out as a modern and ecofriendly approach to accelerate organic reactions. This method minimizes the formation of waste and avoids the use of toxic solvents and reagents. Overall, microwave allows conducting cleaner reactions with improved yields and stereoselectivity.

We previously described a microwave-assisted synthesis of (2E)-2-(5-substituted 2-thienylmethylene)-4-arylbutanamides and (2E,3Z)-4-hydroxy-4-aryl-2-(5-substituted thien-2-yl-methylene)but-3-enohydrazide derivatives [18], which showed pronounced antimicrobial and in vitro cytotoxic activity (IC50) against hu-

man breast carcinoma cell line (using flourouracil as a reference drug) in the cytotoxicity assay developed by Skehan [19].

The aim of the present work is to synthesize a novel antitumor and antimicrobial product, i.e., hydroxypyrrolidin-2-one, which is expected to possess potent antitumor properties. A thorough crystallographic, spectroscopic, and computational analysis was performed to establish its stereochemistry, chemical characterization, and molecular structural features. Single crystal X-ray studies are particularly useful to obtain essential information such as the molecular geometry, bond distances and angles, and packing of the molecules in the crystal. Furthermore, it allows determining the absolute configuration through the identification of small diffraction intensity differences between two crystal structures [20].

**Experimental.** *General remarks.* Microwave irradiation was performed using a Galanz microwave oven, WP1000AP30-2, in the Chemistry Department, Faculty of Women for Arts, Science, and Education, Ain Shams University. IR spectra were conducted at Micro Analytical Center, Ain shams University, using a PERKIN-ELMER-1430 instrument. MS spectra were carried out at Micro Analytical Center, Al-Azhar University, using a GCMS QP 1000 EX Shimadzu device. $^1$H NMR spectra were recorded using a Varian Gemini (300 MHz) at the main Chemical Warfare Laboratories, Chemical Warfare Department, Ministry of Defense. Antimicrobial screening was measured at the Botany Department, Al-Azhar University. Cytotoxic measurements were performed at the Botany Department, Al-Azhar University. Crystallographic data was measured at Elettra–Sincrotrone Trieste, S. S. 14 Km 163.5 in Area Science Park, 34149 Basovizza–Trieste, Italy.

*Catalyst- and solvent-free microwave synthesis of (3E)-5-hydroxy-1-isopropyl-3-[(5-methyl-2-thienyl)methylene]-5-phenylpyrrolidin-2-one.* In a microwave oven (1000 watt, 30–80% of its total power), a grind mixture of (3E)-3-[(5-methyl-2-thienyl)methylene)-5-phenylfuran-2(3H)-one (**1**) [21, 22] (1 mol) and isopropylamine (2 moles) in the presence or absence of dimethyl formamide (DMF) was irradiated in an open vessel for 3–20 min. Completion of the reaction was confirmed by thin layer chromatography. The reaction mixture was then cooled down to room temperature, and the product obtained was dissolved in methylene chloride, followed by washing of the organic layer several times with dilute hydrochloric acid to remove unreacted amine. The organic layer was thoroughly washed with water and dried over anhydrous sodium sulfate. Subsequent distillation of the solvent and recrystallization from benzene/petroleum ether (40/60) gave (3E)-5-hydroxy-1-isopropyl-3-[(5-methyl-2-thienyl)methylene]-5-phenylpyrrolidin-2-one (**2**) as brown crystals in 96.02% yield; m.p. 165–167°C. The chemical structure was confirmed by IR, $^1$H NMR, MS, and X-ray crystallography. The reaction mechanism is shown in Scheme 1.

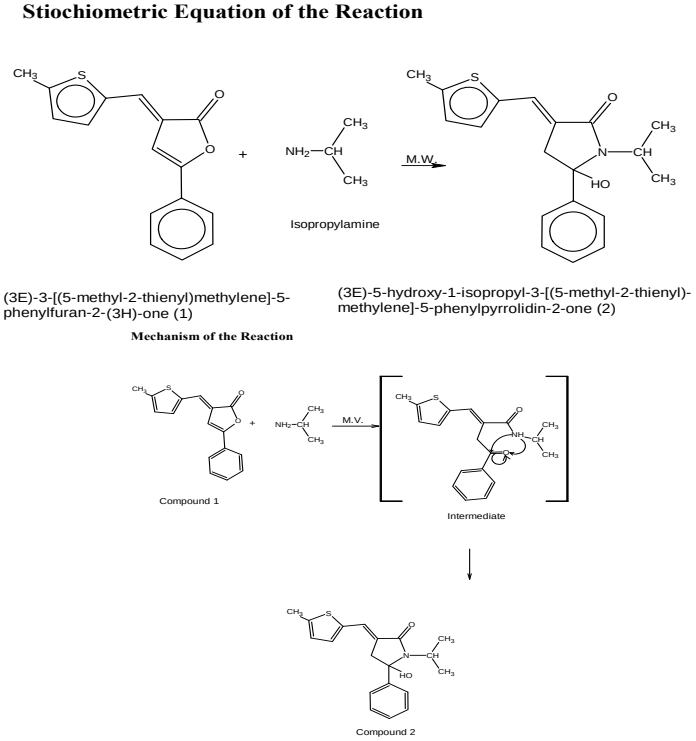


Scheme 1. Mechanism of the synthetic reaction.

*Spectral data.* FTIR (KBr): ν ($cm^{-1}$) = 3345 (OH, hydroxy), 1671 (CO, lactam). MS: *m*/*z* = 327 ($M^+$, 9.11%, $C_{19}H_{21}NO_2S$), 326 (17.47, $C_{19}H_{20}NO_2S$), 325 (8.91, $C_{19}H_{19}NO_2S$), 313 (14.74, $C_{18}H_{19}NO_2S$), 312 (10.56, $C_{18}H_{18}NO_2S$), 308 (5.35, $C_{19}H_{18}NOS$), 307 (3.70, $C_{19}H_{17}NOS$), 284 (5.45, $C_{17}H_{18}NOS$), 250 (2.89, $C_{13}H_{16}NO_2S$), 232 (11.46, $C_{13}H_{14}NOS$), 60 (100, $C_2H_6NO$). $^1$H NMR (DMSO-$d_6$): δ (ppm) = 9.110 (1H, s, H-9), 7.826–7.818 (2H, d, H-6), 7.488–7.477 (1H, d, H-3), 7.378–7.338 (2H, t, H-7), 7.258 (1H, s, H-4), 7.204–7.112 (1H, t, H-8), 6.899–6.891 (1H, d, H-2), 3.728–3.641 (2H, m, H-5), 2.552 (3H, s, H-1), 2.493–2.298 (1H, septet, H-10), 1.548–1.301 (3H, d, H-11), and 1.301–1.007 (3H, d, H-12).

*X-ray crystallography.* Data collections were performed at the X-ray diffraction beamline (XRD1) of the Elettra Synchrotron (Trieste, Italy) [23]. Orange rods were obtained upon slow evaporation from benzene solution. Crystals were dipped in NHV oil (Jena Bioscience GmbH) and mounted on the goniometer head with a nylon loop. Complete datasets were collected at room temperature through the rotating crystal method. Data were acquired using a monochromatic wavelength of 0.700 Å on a Pilatus 2M hybrid-pixel area detector. The diffraction data were indexed and integrated using XDS [24]. The structures were solved by the dual space algorithm implemented in the SHELXT code [25]. Structure refinement, analysis, and presentation of the results were performed using the CRYSTALS program [26] and the general-purpose crystallographic tool PLATON [27]. The molecular graphics were generated using ORTEP-3 for Windows [28] and DIAMON [29] programs. Essential crystal data are summarized in Table 1. CCDC 1577284 contains the supplementary crystallographic data for the title compound. These data can be obtained free of charge from the Cambridge Crystallographic Data Center via https://www.ccdc.cam.ac.uk/structures.

**Results and discussion.** *Structure description.* The structural formula of the novel antitumor and antimicrobial compound **2** was confirmed by crystallographic and spectroscopic characterization. An X-ray single crystal diffraction analysis revealed that the compound crystallized in a centrosymmetric orthorhombic space group with *Z* = 8 and *E*-configuration. The molecular geometry was also calculated using density functional theory (DFT) calculations. A good agreement was observed between the experimental and theoretical geometry parameters, with minor variation in few bond lengths and angles. Moreover, the molecular electrostatic potential was calculated, finding that the most electrophilic site was located near the OH group attached to heterocyclic ring, which is consistent with the bioactivity results. The frontier molecular orbitals were also determined, affording an energy difference between the highest occupied molecular orbital (HOMO) and the lowest unoccupied molecular orbital (LUMO) of –0.15228 eV. On the basis of the results, we proposed a mechanism in which an intramolecular nucleophilic attack occurs on the carbonyl carbon by the lone pair of electrons on the nitrogen atom, resulting in ring closure, proton transfer to oxygen, and formation of the hydroxyl group.

Figure 1 shows an ORTEP diagram of hydroxypyrrolidin-2-one **2**, which was crystallized as a racemic mixture in the orthorhombic *Pbca* space group with one molecule in the asymmetric unit, as summarized in Table 1.

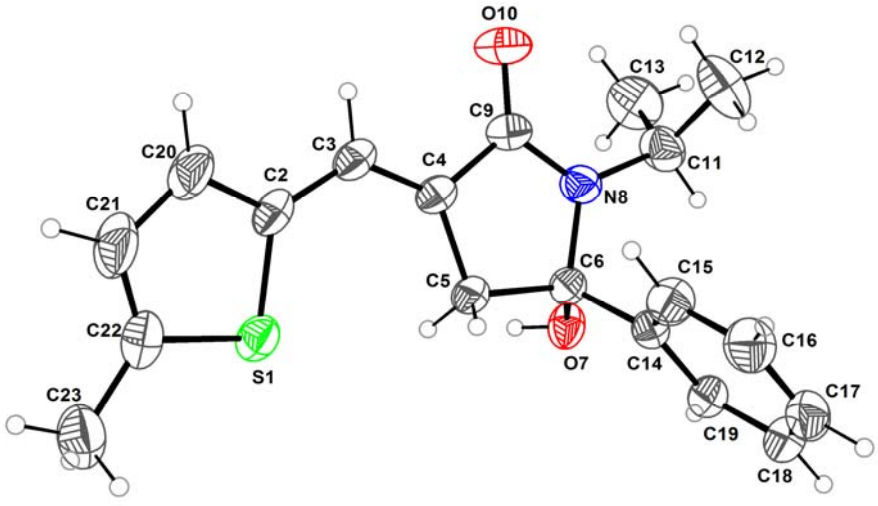


Fig. 1. ORTEP representation of compound **2**, showing the atom labeling scheme. Displacement ellipsoids are drawn at the 50% probability level.

TABLE 1. Crystal Data of the Title Compound

| Chemical formula | $C_{19}H_{21}NO_2S$ |
|---|---|
| $M_r$, Da | 327.45 |
| Crystal system, space group | Orthorhombic, *Pbca* |
| Temperature, K | 298 |
| *a*, *b*, *c*, Å | 10.701 (2), 9.753 (2), 33.507 (7) |
| *V*, Å$^3$ | 3497.0 (12) |
| *Z* | 8 |
| Radiation type | Synchrotron, λ = 0.70000 Å |
| Crystal size, mm | 0.11×0.10×0.06 |
| No. of measured, independent and observed [$I$>2.0σ($I$)] reflections | 48578, 6306, 5667 |
| Refinement | |
| $R[F^2>2\sigma(F^2)]$, $wR(F^2)$, $S$ | 0.055, 0.125, 1.04 |
| Data, restraints, parameters | 5667, 1, 211 |
| $\Delta\lambda_{max}$, $\Delta\lambda_{min}$, e Å$^{-3}$ | 0.29, −0.40 |

The results obtained show that the structure was centered mainly on the pyrrolidine ring of the 5-hydroxypyrrolidin-2-one moiety, with the N8 atom attached to the isopropane group and the C6 atom bonded with the phenyl ring and the hydroxyl group. The consistency of the geometrical parameters of the structure was performed through MOGUL and Cambridge Structural Database (CSD) [30]; the bond lengths and angles of both structures were in good agreement with each other and also with predetermined structures having similar moieties. However, MOGUL reported unusual angles at the pyrrolidine ring and its attached moieties, such as 112.69° for O7–C6–C5 and 110.43° for C14–C6–N8 (Fig. 1), being the difference between those values and the nearest angle in the MOGUL distribution ($d_{min}$) 0.16° and 0.73°, respectively. The MOGUL search was based on the choice of exact fragments in CSD considering that the unusual report of exact fragments must be less than 15 for bonds, angles, and rings, and 40 for torsion angles. The unusual angles could be explained in terms of steric hindrance and packing effect.

The individual moieties exhibit planar configuration, in which the least-squares plane passing through S1–C2–O1–C20–C21–C22 (thiophene ring), N8–C6–C5–C4–C9 (pyrrolidine ring), and C14–C15–C16–C17–C18–C19 (phenyl ring) show a maximum deviation of 0.013(1) Å for N8. However, the phenyl ring plane is nearly perpendicular (89.8°) to the plane crossing the other moieties (Fig. 2). The obtained structure showed good agreement with the calculation results (Fig. 3). In the title compound, the crystal structure packing forms networks stabilized by intermolecular hydrogen bonds, C—H…O (Table 2). The crystal packing is further stabilized by a pi-ring (Cg) stacking interaction C9—O10…Cg, where Cg refers to the center of gravity for the five-membered ring formed by N8–C6–C5–C4–C9 (Fig. 3). No solvent molecules were found in the crystal packing. The results reveal that the molecule contains two centers of chirality (Fig. 3), i.e., the carbon atom attached to the –OH group, the phenyl ring, –$CH_2$, and the nitrogen atom and the nitrogen atom attached to the carbonyl carbon, the isopropyl group, the chiral carbon, and the $sp^3$ lone pair of electrons.

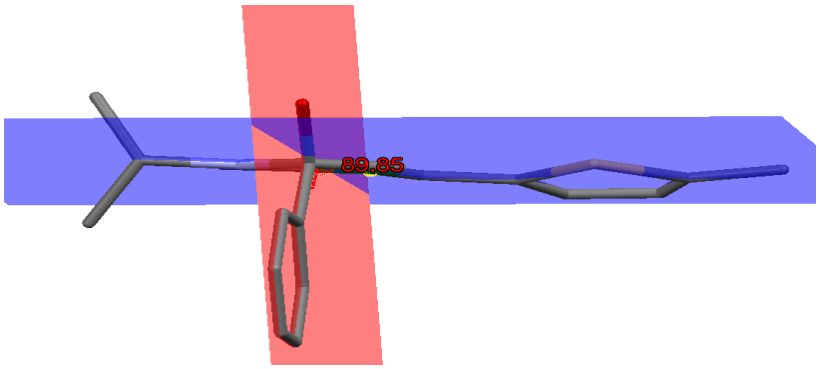


Fig. 2. A view of the structure of **2** showing the phenyl ring orientation.

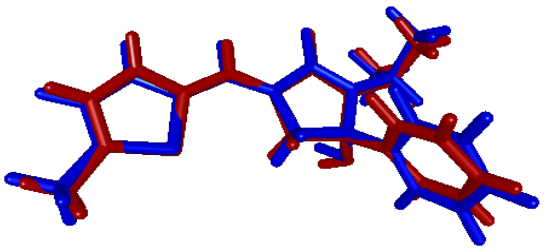

Fig. 3. Overlay view of the X-ray (red) and DFT structure (blue).

TABLE 2. Intermolecular Contacts (Å, degree) of the Structure

| *D*—H···*A* (degree) | *D*···*A* (Å) | H···*A* (Å) | *D*—H (Å) | *D*—H···*A* |
|---|---|---|---|---|
| 134.88 (3) | 3.265 (1) | 2.525(1) | 0.95(1) | C5—H51···O10[a] |
| Y—X…Cg (degree) | Y…Cg (Å) | X…Cg (Å) | Y—X (Å) | Y—X…Cg |
| 120.62 (7) | 4.344(1) | 3.583(1) | 1.24(1) | C9—O10···Cg[b] |

Symmetry code(s): [a] $x + 1/2, y + 1/2, z$. [b] $1/2 - X, -1/2 + Y, Z$.

*Computational measurements.* The molecular structure of the studied molecule (Fig. 4) in the ground state was optimized using DFT (DFT/B3LYP) [31, 32] method with the 6-31G(*d*,*p*) basis set [33]. All the calculations were performed using Gauss View 05 molecular visualization program and Gaussian 09 program package [34, 35].

*Molecular electrostatic potential (MEP).* MEP is a good tool for identifying the reactive sites toward positively or negatively charged reactants, allowing to establish the hydrogen bonding and structure–activity relationships of the molecule; however, the molecular charge distribution remains unperturbed through the external test charge [36]. Quantum chemical calculations have revealed that there is a strong correlation between the dipole moment, electronegativity, and partial charges and the electrostatic potential [37]. MEP provides a visual method to understand the relative polarity of a molecule through mapping the total density surface on the electrostatic potential energy surface, depicting the size, shape, charge density, and reactive sites of the molecules.

The MEP plots of the title compound shown in Fig. 5. In this molecule, the regions near the double bonded oxygen atom of the five-membered heterocyclic ring are the most electrophilic site (red regions) due the concentrated electron density. The oxygen atom of the OH group attached to the heterocyclic ring represents others electrophilic site. The regions near the sulfur atom (blue regions) represent the nucleophilic site of the studied molecule.

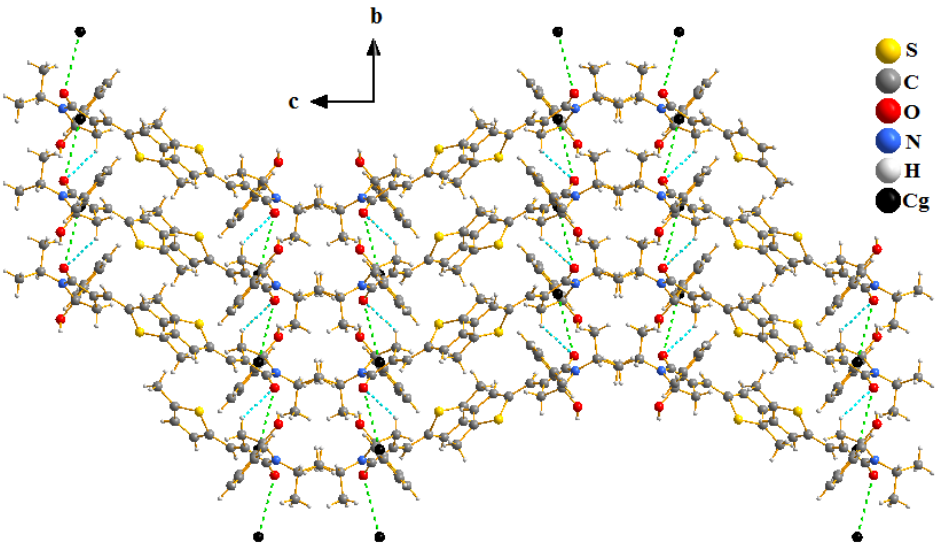


Fig. 4. Packing view along the *a*-axis, showing the intermolecular contacts (dashed lines) of the structure of **2**.

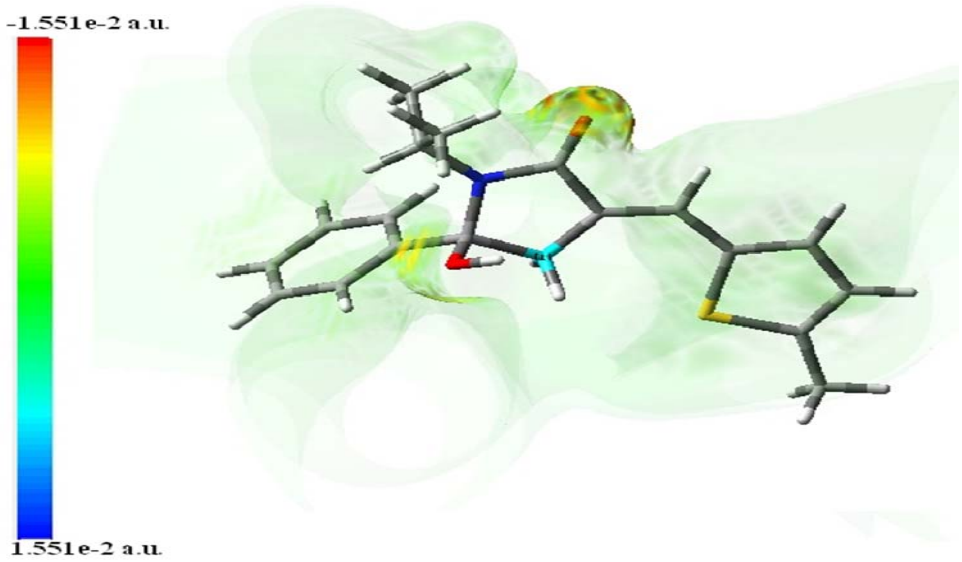


Fig. 5. Molecular electrostatic potential mapped on the isodensity (total density) surface from $-1.551 \cdot 10^{-2}$ to $+1.551 \cdot 10^{-2}$ a.u.

*Frontier molecular orbitals (FMOs)*. The electronic transition occurs from the electron-donating HOMO to the electron-accepting LUMO. Both FMOs are the main orbitals involved in the chemical reaction. The electron delocalization between these orbitals is a principal factor determining the easiness and stereoselectivity of a chemical reaction, either for intra- or intermolecular processes. Furthermore, the energy gap between HOMO and LUMO characterizes the chemical reactivity, kinetic stability, and spectroscopic properties of molecules [38]. The FMOs of the present molecule were computed at the B3LYP/6-31G(*d*,*p*) level. The results are shown in Fig. 6, together with the energy levels.

The negative values of the FMO energies indicate the stability of the studied molecule. The double bonded oxygen atom in the five-membered heterocyclic ring mainly contributes to the HOMO of hydroxypyrrolidinone **2**, whereas the sulfur atom essentially participates in the LUMO. The energy gap between HOMO and LUMO is −0.15228 eV, which is indicative of the good thermodynamic stability of the compound.

The results obtained led us to propose a reaction mechanism in which a ring closure occurs through an intramolecular nucleophilic attack by the lone pair of electrons on the nitrogen atom to the carbonyl carbon, with the concomitant proton transfer to the negatively charged oxygen (Scheme 1). The *E*-configuration of the double bond is preserved from the starting material, and the product is a racemic mixture.

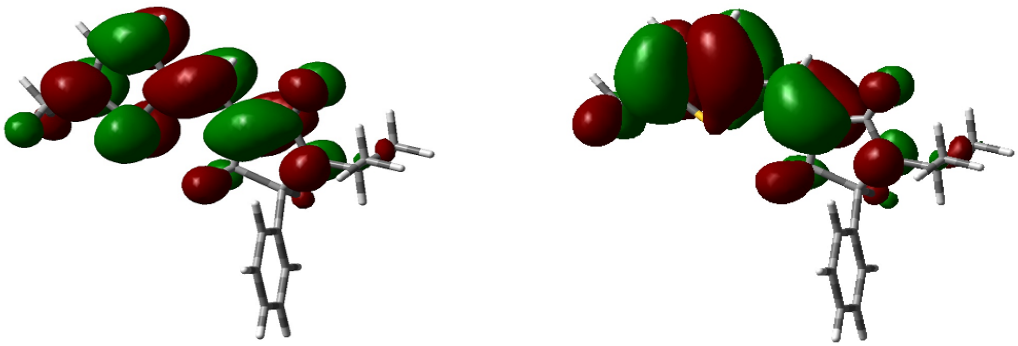

LUMO (–0.05819 eV) HOMO (–0.21047 eV)

Fig. 6. Molecular orbital surfaces and energy levels given in parentheses for the HOMO and LUMO of compound **2** computed by B3LYP/6-31G(*d*,*p*) method.

**Medicinal and biological activities.** The *in vitro* antiproliferative activity (IC50) of compound **2** against a human breast carcinoma cell line (MCF-7) and a human colon carcinoma cell line (HCT-116) was evaluated using doxorubicin or cisplatin as a reference drug, following the procedure reported by Skehan et al. [19]. IC50 is defined as the concentration that results in a 50% decrease in cell number as compared with that of control structures in the absence of an inhibitor. The results obtained are given in Table 3 and Fig. 7.

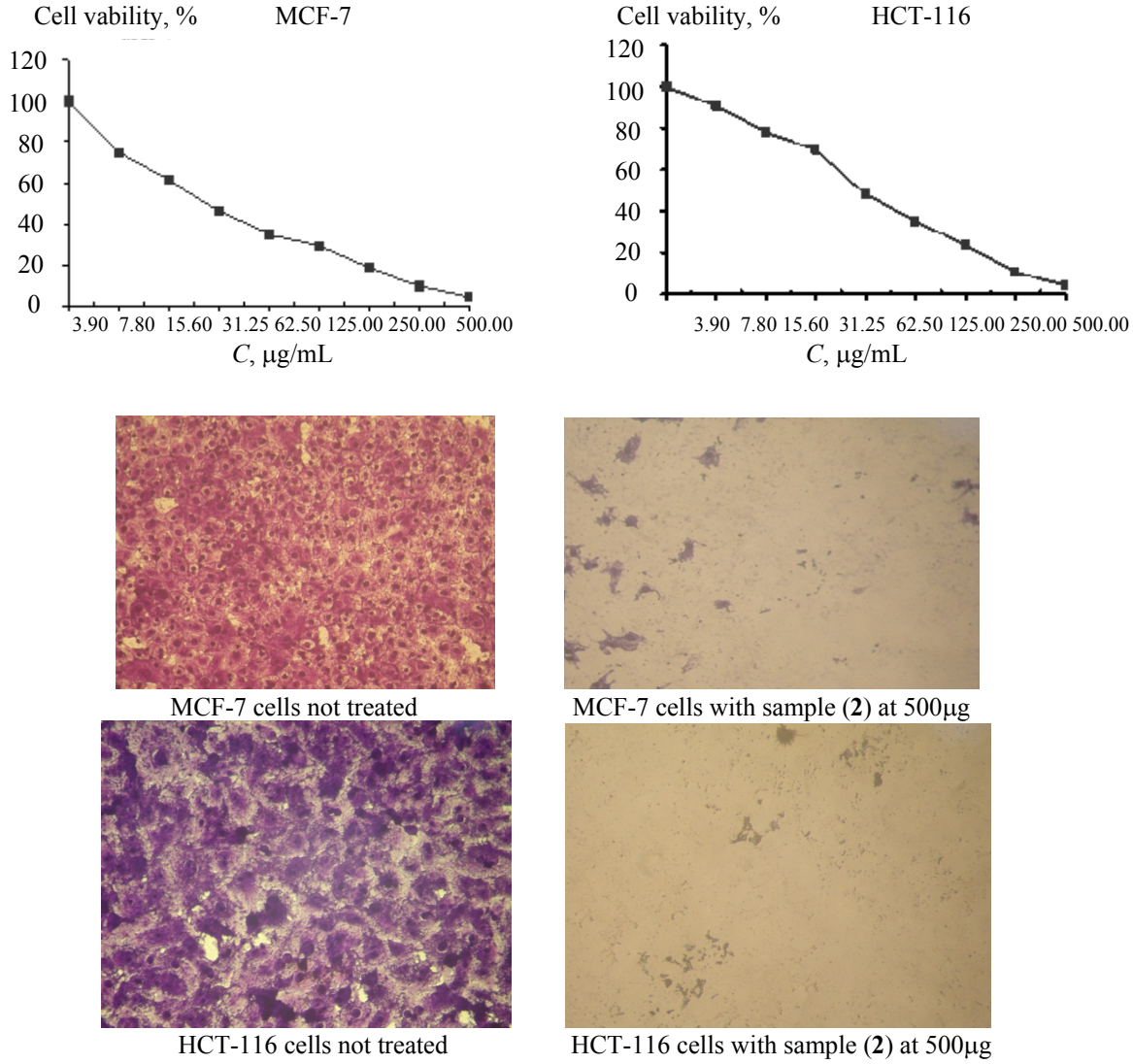


Fig. 7. *In vitro* antiproliferative activity (IC50) of compound **2** against a human breast carcinoma cell line and a human colon carcinoma cell line.

The antimicrobial screening of compound **2** was performed using the disk diffusion method with an inhibition zone (mm/mg) in DMSO as solvent. The compound exhibited antimicrobial activity ranging from high to moderate against *Bacillus subtilis* (G+), *Staphylococcus aureus* (G+), *Escherichia coli* (G−), and *Pseudomonas aeruginosa* (G−). The results obtained are presented in Table 3.

TABLE 3. Cytotoxic Activity and Antimicrobial of Compound **2**

| Antitumor activity IC50 μg/ml | | Gram negative bacteria | | Gram positive bacteria | | Fungi | | Compound No. |
|---|---|---|---|---|---|---|---|---|
| HCT-116 | MCF-7 | Pseudomonas aeruginosa (RCMB 010043) | Escherichia coli (RCMB 010052) | Staphylococcus aureus (RCMB 010028) | Streptococcus pneumoniae (RCMB 010010) | Candida albicans (RCMB 05036) | Aspergillus fumigatus (RCMB 02568) | |
| 2.3 | 1.2 | NA | 23.1±0.63 | 25.3±1.5 | 22.6±0.58 | 21.3±0.63 | 23.2±1.2 | 2 |
| Doxorubicin or cisplatin | | Gentamycin 20.6±1.2 | Gentamycin 23.4±0.63 | Ampicillin 27.4±0.72 | Ampicillin 23.8±1.2 | Amphotericin B 25.4±0.58 | Amphotericin B 23.7±1.2 | Reference drug |

**Conclusions.** The title compound was synthesized efficiently with assistance of microwave irradiation, and its structure was confirmed by crystallographic and spectroscopic characterization. Its antitumor and antimicrobial activities were evaluated. The X-ray crystallography revealed that the compound crystallized in an orthorhombic centrosymmetric crystal form, with unambiguous assignment of the *E*-configuration for the $C_3$–$C_{thienyl}$ bond. The molecular geometry was also optimized using DFT, which was in good agreement with the experimental data. The calculated MEP suggests that the most electrophilic site locates near the OH group attached to the heterocyclic ring, which is consistent with the bioactivity results. The FMOs were also determined, being the energy difference between HOMO and LUMO of –0.15228 eV. The following mechanism is proposed: an intramolecular nucleophilic attack occurs on the carbonyl carbon by the lone pair of electrons on the nitrogen atom, leading to ring closure with the concomitant proton transfer to oxygen, which results in the formation of the hydroxyl group. The microwave irradiation technique proved to be environmentally safe and rapid, affording the product in high yield and purity. Such requirements are essential for the synthesis of medicinal and bioactive compounds. The combination of X-ray diffraction techniques, spectroscopic methods, and DFT calculations proved highly effective for elucidating the structure and properties of the studied compound, thereby providing important information for the pharmaceutical community for the design and manufacture of effective anticancer drugs.

There are no conflicts to declare.

**Acknowledgments.** We thank Dr. El Sayed Shalaby (Elettra–Sincrotrone Trieste, Italy & Crystallography Lab., NRC, Egypt) for the great help during X-ray diffraction data collection and crystal structure refinement. We thank Dr. Shadia M. Abdallah, Associate professor of Organic Chemistry, Department of Chemistry, Faculty of Women for Arts, Science, and Education, Ain Shams University, Cairo, Egypt, for her great help during this work.

## REFERENCES

1. V. O. Koz'minykh, N. M. Igidov, S. S. Zykova, V. É. Kolla, N. S. Shuklina, T. F. Odegova, *Pharm. Chem. J.*, **36**, 188–191 (2002).
2. T. Michael, A. Michael, T. Andreas, H. Ulrich, B. Mirko, N. A. Johannes, Patent WO2008055945(A1) (2008).
3. Y. Geng, X. Wang, L. Yang, H. Sun, Y. Wang, Y. Zhao, R. She, M.-X. Wang, D.-X. Wang, J. Tang, *PLoS One*, **10**, 1–15 (2015).
4. A. Pendri, T. L. Troyer, M. J. Sofia, M. A. Walker, B. N. Naidu, J. Banville, N. A. Meanwell, I. Dicker, Z. Lin, M. Krystal, S. W. Gerritz, *J. Comb. Chem*., **12**, 84–90 (2010).
5. K. Ma, P. Wang, W. Fu, X. Wan, L. Zhou, Y. Chu, D. Ye, *Bioorg. Med. Chem. Lett.*, **21**, 6724–6727 (2011).
6. V. L. Gein, M. N. Armisheva, N. A. Rassudikhina, M. I. Vakhrin, E. V. Voronina, *Pharm. Chem. J.*, **45**, 162–164 (2011).
7. V. L. Gein, V. A. Mihalev, N. N. Kasimova, E. V. Voronina, M. I. Vakhrin, E. B. Babushkina, *Pharm. Chem. J.*, **41**, 208–210 (2007).
8. V. L. Gein, V. V. Yushkov, N. N. Kasimova, N. S. Shuklina, M. Y. Vasil'eva, M. V. Gubanova, *Pharm. Chem. J.*, **39**, 484–487 (2005).
9. M. S. F. Franco, G. A. Casagrande, C. Raminelli, S. Moura, M. Rossatto, F. H. Quina, C. M. P. Pereira, A. F. C. Flores, L. Pizzuti, *Synth. Commun*., **45**, 692–701 (2015).

10. M. Anada, S. Hashimoto, *Tetrahedron Lett*., **39**, 79–82 (1998).
11. D.-R. Choi, K.-Y. Lee, Y.-S. Chung, J.-E. Joo, Y.-H. Kim, C.-Y. Oh, Y.-S. Lee, W.-H. Ham, *Arch. Pharm. Res*., **28**, 151–158 (2005).
12. L. E. Burgess, A. I. Meyers, *J. Org. Chem*., **57**, 1656–1662 (1992).
13. L. E. Overman, T. P. Remarchuk, *J. Am. Chem. Soc*., **124**, 12–13 (2002).
14. V. Singh, R. Saxena, S. Batra, *J. Org. Chem.*,**70**, 353–356 (2005).
15. R. Sarkar, C. Mukhopadhyay, *Tetrahedron Lett*., **54**, 3706–3711 (2013).
16. J. Sun, Q. Wu, E.-Y. Xia, C.-G. Yan, *Eur. J. Org. Chem*., **16**, 2981–2986 (2011).
17. Q. Zhu, H. Jiang, J. Li, S. Liu, C. Xia, M. Zhang, *J. Comb. Chem*., **11**, 685–696 (2009).
18. B. M. Awad, H. A. Saad, E. M. Nassar, E. M. Azmy, *J. Am. Sci*., **9**, 566–577 (2013).
19. P. Skehan, R. Storeng, D. Scudiero, A. Monks, J. McMahon, D. Vistica, J. T. Warren, H. Bokesch, S. Kenney, M. R. Boyd, *J. Natl. Cancer Inst*., **82**, 1107–1112 (1990).
20. H. D. Flack, G. Bernardinelli, *Chirality*, **20**, 681–690 (2008).
21. N. R. Guirguis, B. M. Awad, H. A. Saad, *J. Prakt. Chem*., **332**, 414–418 (1990).
22. N. R. Guirguis, B. M. Awad, H. A. Saad, *Liebigs Ann. Chem.*, No. 6, 1003–1011 (**1986**).
23. A. Lausi, M. Polentarutti, S. Onesti, J. R. Plaisier, E. Busetto, G. Bais, L. Barba, A. Cassetta, G. Campi, D. Lamba, A. Pifferi, S. C. Mande, D. D. Sarma, S. M. Sharma, G. Paolucci, *Eur. Phys. J. Plus*., **130**, 1–8 (2015).
24. W. Kabsch, *Acta Crystallogr. Sect. D Biol. Crystallogr.*, **66**, 125–132 (2010).
25. G. M. Sheldrick, *Acta Crystallogr. Sect. A Found. Adv.*, **71**, 3–8 (2015).
26. P. W. Betteridge, J. R. Carruthers, R. I. Cooper, K. Prout, D. J. Watkin, *J. Appl. Crystallogr.*, **36**, 1487–1489 (2003).
27. A. L. Spek, *Acta Crystallogr. Sect. D Biol. Crystallogr*., **65**, 148–155 (2009).
28. L. J. Farrugia, *J. Appl. Crystallogr*., **45**, 849–854 (2012).
29. K. Brandenburg, Cryst. Impact GbR (2012).
30. I. J. Bruno, J. C. Cole, M. Kessler, J. Luo, W. D. S. Motherwell, L. H. Purkis, B. R. Smith, R. Taylor, R. I. Cooper, S. E. Harris, A. G. Orpen, *J. Chem. Inform. Comput. Sci*., **44**, 2133–2144 (2004).
31. R. Ditchfield, W. J. Hehre, J. A. Pople, *J. Chem. Phys*., **54**, 724–728 (1971).
32. A. D. Becke, *J. Chem. Phys*., **98**, 5648–5652 (1993).
33. J. B. Foresman, A. Frisch, *Exploring Chemistry with Electronic Structure Methods*, Gaussian, Inc, Pittsburgh, P.A. (1996).
34. *Gaussian09, Rev*., Gaussian, Inc., Wallingford CT (2009).
35. A. Frisch, A. B. Nielson, A. J. Holder, *Gauss View User Manual*, Gaussian Inc., Pittsburgh, Pennsylvania (2005).
36. B. D. Joshi, R. Mishra, P. Tandon, A. C. Oliveira, A. P. Ayala, *J. Mol. Struct*., **1058**, 31–40 (2014).
37. Munoz-Caro, Nino, Senent, Leal, Ibeas, *J. Org. Chem*., **65**, 405–410 (2000).
38. S. Radhakrishnan, R. Parthasarathi, V. Subramanian, N. Somanathan, *Comput. Mater. Sci*., **37**, 318–322 (2006).